The possibility of angiogenesis inhibition in cutaneous melanoma by Bevacizumab-loaded lipid-chitosan nanoparticle

fershteh Abdi
Kermanshah University of Medical Sciences
Elham Arkan
Kermanshah University of Medical Sciences
Mojtaba Eidizadeh
Kermanshah University of Medical Sciences
Elahe Valipour
Kermanshah University of Medical Sciences
Tahereh Naseriyeh
Kermanshah University of Medical Sciences
Younes Hossainy Gamizgy
Kermanshah University of Medical Sciences
Kamran Mansouri (kamranmansouri@gmail.com)
Kermanshah University of Medical Sciences

Research Article

Keywords: cutaneous melanoma, Bevacizumab, angiogenesis, lipid-polymer nanoparticle, local drug delivery

Posted Date: April 8th, 2022

DOI: https://doi.org/10.21203/rs.3.rs-1450723/v1

Abstract

Cutaneous malignant melanoma is fastest-growing cancer in white populations with a large majority of dermal cancer death. The activity of vascular endothelial growth factors (VEGFs) results in the signaling of a variety of downstream intracellular pathways that ultimately leads to cell activation, proliferation, migration, and angiogenesis. VEGF inhibitors such as Bevacizumab are widely used in chemotherapy with systemic administration, which in many cases is associated with a variety of side effects. Here, we designed and synthesized a lipid-polymer nanoparticle for local administration of Bevacizumab. Drug release, dermal absorption, and the effects of synthesized nanoparticles containing Bevacizumab on cell proliferation and in vitro and in vivo angiogenesis were investigated. Encapsulating Bevacizumab in the synthesized nanoparticles resulted in a significant increase in its dermal absorption compared to free Bevacizumab. Also, the suppressor effects of Bevacizumab encapsulated in the synthesized nanoparticle on cell proliferation and angiogenesis were significantly more than those of free Bevacizumab. Our findings indicate the remarkable effects of lipid-polymer nanoparticles in dermal absorption and in maintaining Bevacizumab bioactivity, suggesting therapeutic benefits of local Bevacizumab administration for angiogenesis-related disorders such as cutaneous melanoma.

1. Introduction

Cutaneous melanoma is a common malignancy with an increasing incidence that develops from pigment-producing cells in skin, melanocytes [1]. The major risk factors in the development of cutaneous melanoma include exposure to UV radiation from the sun or other sources, chronic dermal lesions such as nevus, a positive family history of melanoma, and poor immune function[2]. Also, several rare skin-related genetic conditions such as xeroderma pigmentosum increase the risk of cutaneous melanoma.

Like other malignancies, angiogenesis plays a vital role in tumor growth, spread, and metastasis of cutaneous melanoma [3]. Angiogenesis, the formation of new blood vessels from existing ones, occurs when the balance between stimuli and inhibitors of angiogenesis is shifted toward stimuli. A variety of angiogenic stimuli have been identified, including vascular endothelial growth factor (VEGF), fibroblast growth factor-B (bFGF), platelet-derived growth factor (PDGF), and transforming growth factors α and β (TGFα/β) [4]. VEGF-A activates several downstream intracellular signaling pathways, including PLCγ, PI3K, and MAPK, by binding to tyrosine kinase receptor-2 (VEGFR-2, also known as Flk-1 and KDR), resulting in an increase in cell proliferation, migration and survival as well as angiogenesis [5, 6].

Bevacizumab is a recombinant monoclonal anti-VEGF antibody commonly used in combination with chemotherapy to prevent tumor angiogenesis and metastasis [7]. Nevertheless, a variety of side effects have been reported for systemic administration of Bevacizumab such as gastrointestinal ulceration [8], cardiovascular disorders[9, 10], hypertension[11], thromboembolic [12, 13], central nervous system hemorrhage [14], and nasal septum perforation [15]. Availability of cutaneous melanoma tumors is an incentive for the local drug injection to eliminate the side effects of systemic administration. Bevacizumab is a water-soluble compound with poor dermal absorption. In addition, the possibility of

denaturation of protein structure by enzymes in the skin and its loss of function are of the challenges of local injection of free Bevacizumab.

Lipid compounds have recently attracted much attention for the local administration of a variety of drugs in skin complications. The effect of lipid-based nanoparticles such as lecithin on increasing the penetration and absorption of water-soluble compounds in the skin has been reported in various studies [16–19]. Furthermore, biodegradable polymers such as chitosan can encapsulate proteins and protect them against environmental enzyme damage [20, 21]. In this study, we designed and synthesized a polymer-lipid nanoparticle (polymer core and lipid coating) that could efficiently load Bevacizumab, increased dermal absorption of Bevacizumab and inhibit angiogenesis in vitro and in vivo.

2. Materials And Methods

2.1 Materials

Chitosan was purchased from Sigma-Aldrich (Germany), Bevacizumab was procured from Ariogen Pharmed (Iran)., triphosphate(TPP), acetic acid, NaOH, lecithin, cholesterol, chloroform, PBS buffer, MTT salt, DMEM medium, FBS, Cytodex 3 microcarriers, 8-day-old eggs, formaldehyde, glyceryl monostearate, vaseline, polysorbate 80, glycerin, Dextran 40, Ethyl p-hydroxybenzoate, Pentylene Glycol, distilled water.

2.2. Synthesis of lipid-coated chitosan-Bevacizumab nanoparticles (Lip-Chi-Bev NPs)

Chitosan nanoparticles were synthesized using the ion exchange method [22]. To prepare 0.05% w/v chitosan solution, 50 mg of chitosan was dissolved in 100 ml of 1% acetic acid and adjusted to pH 6. Chitosan nanoparticles were prepared by adding 1 mL of TPP solution (0.2 mL per min) to 3 mL of chitosan solution under stirring at 900 rpm. Chitosan nanoparticles containing Bevacizumab (Chi-Bev NPs) were synthesized by stirring 3 mg of Bevacizumab with 3 ml of chitosan solution for one hour at 300 rpm. Then, 1 ml of TPP solution at 900 rpm/0.2ml per min were added to the chitosan solution containing Bevacizumab. The prepared chitosan nanoparticles were then lyophilized and stored at 4°C[23]. To lipid-coating the chitosan nanoparticles containing Bevacizumab (Lip-Chi-Bev NPs), 16 mg of chitosan nanoparticles containing Bevacizumab (10 mg Bevacizumab) was dispersed in 50 ml of 45°C water. Then, 18 mg lecithin and 2mg cholesterol were dissolved in 600µl of chloroform, and rotated at 50°C, 100rpm. An hour later, a thin lipid film was formed, and an aqueous solution containing chitosan nanoparticles was then added to that and placed in an ultrasonic bath for 5 min, stirred for 45min at 45°C, sonicated for 4 min, and finally placed in an ultrasonic bath for 2 min.

2.3 Characterization of Lip-Chi-Bev NPs

Dynamic light scattering (DLS) was performed to determine the size, polydispersity index (PDI) and zeta potential of Lip-Chi-Bev NPs using a nanosizer instrument (Malvern, England). The exact particle size of Lip-Chi-Bev NP was also confirmed by scanning electron microscopy (SEM) (Quanta450, Fei, United

States). The formation of Chi -Bev NPs, Lip-Chi-Bev NPs and the loading of Bevacizumab into nanoparticles was confirmed by Fourier-transform infrared spectroscopy (FTIR). FTIR spectrum was scanned by Shimadzu IR2000 (Japan) in the range of 400–4000 cm^{-1} and scanning speed of 8/cm for 100 scans.

2.4 Determining the entrapment efficiency and drug loading

First, the entrapment efficiency and drug loading were measured for chi-Bev NPs and then, the final drug loading for Lip-Chi-Bev NPs was evaluated according to the following formulas. So that, the chi-Bev NPs were centrifuged for 30 min at 15,000 rpm, the amount of free Bevacizumab in the supernatant was measured using UV spectroscopy at 278 nm. The resulting precipitate was also lyophilized to obtain the total mass of chi-Bev NPs. After lipid coating of chi -Bev NPs, the final measurement of drug loading was performed, and the precipitated nanoparticles of the centrifuge at 15,000 rpm/45 min were lyophilized to obtain the total mass of Lip-Chi-Bev NPs.

$$\% \text{ Entrapment efficiency} = \frac{\text{AmountofBevacizumabentrapped}}{\text{TotalamountofBevacizumabadded}} \times 100$$

$$\% \text{ Drug loading} = \frac{\text{AmountofBevacizumabentrapped}}{\text{Amountoftotalnanoparticle}} \times 100$$

2.5 Drug release study

27 mg of Lip -Chi-Bev NPs containing 10 mg of Bevacizumab was dispersed in 50 ml PBS buffer and placed in a shaker/incubator 37°C/100 rpm for 48 hours, then removed 1 ml of solution at times of 1, 2, 4, 6, 8, 10, 12, 24 and 48 hours and centrifuged at 12,000 rpm. The supernatant was used to measure the amount of released Bevacizumab, and the precipitate was dissolved in 1 ml of buffer and returned to the original solution. Measurement of released Bevacizumab was done in triplicate. The amount of Bevacizumab in the samples was measured using UV spectroscopy at 278 nm.

2.6 Measurement of dermal absorption

For using animals in the study, the study procedure was approved by the Research Ethics Committee of Kermanshah University of Medical Sciences (IR.SBMU.RETECH.REC.1398.11.11). Evaluation of dermal absorption of Lip-Chi-Bev NPs was performed once alone and once in a cream base to facilitate the final application. To evaluate the dermal absorption of Lip-Chi-Bev NPs, a two-phase cream base (water in oil)is required. Oil phase components (20 g glyceryl monostearate, 2g Vaseline, 0.2g polysorbate 80) and water phase components (25g glycerin, 0.3g Dextran 40, 2g Ethyl p-hydroxybenzoate, 50ml distilled water) were melted separately. The oil phase and the aqueous phase were mixed and pentylene glycol was added as a preservative.

Six-week-old Balb/c mice with weights about 35 g were used to evaluate the dermal absorption of Lip-Chi-Bev NPs. Mice were anesthetized with chloroform and then killed by amputation of the spinal cord. The full-thickness skin of the abdomen was completely removed and kept in normal saline phosphate until use. The isolated skins were applied immediately without storage. 0.05 M buffer (47.5 ml of 0.2 M

NaH2PO4 solution and 202.5 ml of 0.38 M NaHHPO4 solution) was prepared at pH 7.2. The Franz diffusion cell was filled with 30 ml (stirring speed: 70 rpm, temperature: 37 ± 2.5 ˚C), of the prepared buffer, and the dermis (the available area: 1×1 cm^2 as a natural membrane, was fixed on top of that. Then 2.7 mg of Lip-Chi-Bev NPs (contain 1mg Bevacizumab) was dispersed in 1 ml of cream and applied to the dermis. Also, 2.7 mg of Lip-Chi-Bev NPs(contain 1mg Bevacizumab) was suspended in 1 ml of PBS buffer. To measure the dermal absorption of free Bevacizumab, a concentration of 1 mg/ml was prepared in PBS buffer. The sampling process was such that every 1 ml of buffer was removed from the inside of the Franz cell and replaced with 1 ml of buffer. Dermal absorption was measured at 37°C for 24 hours. Under the same conditions, 2.7 mg of Lip-Chi-Bev NPs was dispersed in 1 ml of 0.05 M buffer and examined. The amount of Bevacizumab in the samples was measured using UV spectroscopy at 278 nm.

2.7 Cell proliferation assay using a two-dimensional in vitro model

1.5×10^3 cells/well of serum-starved hBMEC cells (human brain microvascular endothelial cells) were seeded in a 96-well plate and incubated with DMEM medium containing 10% FBS for 48 hours. Four cell groups were considered, including control cells, cells exposed to lipid-coated chitosan nanoparticles without Bevacizumab (Lip -Chi NP), cells exposed to free Bevacizumab, and cells exposed to Lip -Chi-Bev NPs. Different concentrations (0.25, 0.725 and 1.25 mg/ml) for each cell group were studied in triplicates. The cells were treated with 25µl/well (5 mg/ml in PBS buffer) of MTT solution. The precipitated purple-blue formazan crystals were dissolved in 100 µl DMSO. Optical density was measured in the 570 nm wavelength using an ELISA reader 450/630 nm.

2.8 Tube formation assay using a three-dimensional in vitro model

First, Cytodex 3 microcarriers were dispersed in 15 ml of PBS buffer and incubated overnight at 4°C until the cytodex swelled. After sterilization of microcarriers, the supernatant was replaced by a fresh DMEM culture medium. hBMEC cells in the logarithmic growth phase were trypsinized and centrifuged. The cell pellet was suspended in DMEM containing 10% FBS and then mixed with an appropriate number of microcarriers, gently shaked for 4 hours. The cell-coated microcarriers were impregnated with collagen solution. Before collagen coagulation, the resulting solution was aliquoted into a 24-well plate and incubated in an incubator 370C. Cell-coated microcarriers were fit well into collagen. The cell groups were then exposed to different concentrations (0.25, 0.725 and 1.25 mg / ml). After 48 hours of incubation, the cells were observed under a microscope and photographed [24].

2.9 Chorioallantoic Membrane Assay (CAM assay)

8-day-old eggs were used to evaluate angiogenesis in vivo. A window was created on the calcareous surface of the eggs. The four mentioned groups were exposed to different concentrations (0.25, 0.725 and 1.25 mg/egg) of desired compounds and administered into eggs every 48 hours for seven days. On

the seventh day, 400 µl of 10% formaldehyde solution was added to each egg, and after 3 hours the eggs were opened and the membrane was separated [25].

2.10 Statistical analysis

All data were presented as mean ± SD. Data graphs were plotted using the GraphPad Prism software. Statistically significant differences were calculated after analysis of ANOVA followed by Tukey's posthoc test. Values ≤ 0.05 were considered statistically significant. Each point or column represents the mean ± SEM. (n = 3); *p < 0.05, **p < 0.01, ***p < 0.001 and ****p < 0.0001.

3. Result

3.1 Characterization of Lip-Chi-Bev NPs

Chi-Bev NP, Lip-Chi-Bev NP and chitosan nanoparticles without Bevacizumab were synthesized. First, the hydrodynamic diameter size of the nanoparticles was investigated (Table 1). The hydrodynamic diameter size of chitosan nanoparticles without Bevacizumab was 117.63 ± 3.6, while it was 137.33 ± 8.7 and 283.31 ± 6.3 for Chi-Bev NPs and Lip-Chi-Bev NPs, respectively. The increase in nanoparticle size confirms the loading of Bevacizumab by chitosan nanoparticles. The hydrodynamic size of Lip-Chi-Bev NP is 283.31 ± 6.3. This increase in size also indicates the placement of a lipid coating on chitosan nanoparticles[26]. The image obtained by SEM showed spherical morphology of Lip-Chi-Bev NPs. Also the reported size by SEM was 209.27 ± 6.4 (Fig. 1). The zeta potential for chitosan nanoparticles without Bevacizumab, Chi -Bev NPs, and Lip-Chi-Bev NPs was 22 ± 1.5, 17.33 ± 0.61, and 15 ± 1.5 mV, respectively (Table 1). The decrease in zeta potential when loaded with Bevacizumab by chitosan nanoparticles indicates that Bevacizumab has a negative charge[27], indicating that the chitosan nanoparticle was able to load Bevacizumab. Observing the negative value of the zeta potential of Lip-Chi-Bev NP, it can be concluded that the lipid coating is well located on Chi-Bev NP[26].

Table 1
Size, PDI and zeta potential of Chitosan NPs, Chi-Bev NPs and Lip-Chi-Bev NPs

Nanoparticles (NPs)	Size(nm)	PDI	Zeta potential(Mv)
Chitosan NPs	117.6 ± 3.6	0.29 ± 0.02	22 ± 1.51
Chi-Bev NPs	137.33 ± 8.7	0.3 ± 0.08	17.33 ± 0.61
Lip-Chi-Bev NPs	283.31 ± 6.3	0.24 ± 0.01	-15 ± 1.5

FTIR analysis was performed to confirm the formation of Chi-Bev NP and Lip-Chi-Bev NP. The FTIR spectrum is shown in Fig. 2 is related to the formation of Chi -Bev NP. In the spectrum of chitosan polymer, two bands 1577cm^{-1} and 1654cm^{-1} are observed. These bonds are reduced when the chitosan polymer cross-links with the TPP molecule and chitosan nanoparticles are formed. In the spectrum of chitosan nanoparticles containing Bevacizumab, the intensity of these bands has decreased. In addition

to the reduction of these bands, two new packets usually appear during the formation of chitosan nanoparticles. In the chitosan nanoparticle spectrum, two bands have appeared in the region of 1512cm^{-1} and 1617cm^{-1}. Successful loading of Bevacizumab antibodies is also well confirmed in the FTIR spectrum (Fig. 3). The bonds for Bevacizumab are 1570cm^{-1} and 1642cm^{-1}. The decrease in the intensity of these bands in the Chi-Bev NP spectrum confirms that Bevacizumab is loaded into chitosan nanoparticles[28].

The placement of lecithin lipid coating on Chi-Bev NP (Lip-Chi-Bev NP formation) can also be examined by FTIR spectroscopy. In the spectrum of Lip-Chi-Bev NP (Fig. 4), it can be seen that the emerging bands have decreased in the formation of Chi-Bev NP. On the other hand, we see a decrease in the 1738cm^{-1} bond of lecithin, which belongs to the carbonyl group of fatty acids. Also, the 1236cm^{-1} bond, which is related to the lecithin phosphate band, has been reduced, which indicates the interaction of lecithin with Chi-Bev NP[29].

3.2 Entrapment and loading efficiency

After confirming the formation of Lip-Chi-Bev NPs and Chi-Bev NPs, and loading Bevacizumab, the efficiency of drug loading and entrapment was measured, which respectively were 62%±3.8 and 75%± 5.1 for Bevacizumab in Chi-Bev NPs. The encapsulation efficiency of Lip-Chi-Bev NPs was 37.03%±2.84.

3.3 Drug release study

The release rate of Bevacizumab was measured at 1, 2, 4, 6, 8, 16, 24, and 48 hours at physiological pH. It was found that the release of the drug follows first-order kinetics. The release of Bevacizumab from Lip-Chi-Bev NPs was 62%±2.15 after 24 hours, and 74%±4.2 after 48 hours (Fig. 5).

3.4 Dermal absorption assay

Dermal absorption of Lip-Chi-Bev NPs was assessed under two conditions, as a suspension in PBS and as dispersed particles in a cream base. Dermal absorption of free Bevacizumab was also evaluated. Dermal absorption was measured after 16 hours for Lip-Chi-Bev NPs suspended in PBS, for Lip-Chi-Bev NPs dispersed in a cream base, and for free Bevacizumab was 72.1% ±1.2, 74.36% ±1.31, and 2.1%±0.03, respectively (Fig. 6). Thereby, Lip-Chi-Bev NPs showed better dermal absorption than free Bevacizumab.

Although the cream base is usually used to increase the stability of nanoparticles and facilitate the application of the desired particles [30], no difference was observed between dermal absorption of Lip-Chi-Bev NPs suspended in PBS and Lip-Chi-Bev NPs dispersed in a cream base. The rate of dermal absorption of Bevacizumab after 16 hours was 78%, indicating an increase not only in the amount released but also in the rate of release of Bevacizumab. The increased antibody release may be due to the good biodegradability of the chitosan polymer [31].

3.5 The effect of Lip-Chi-Bev NPs on cell proliferation

Cell proliferation was examined as a critical process in angiogenesis. After examining cell proliferation in all four mentioned cell groups, no significant difference was observed between cells treated with Lip-Chi NPs and the control cells. Cells treated with Lip-Chi-Bev NPs showed a significant decrease in proliferation rate compared to cells treated with free Bevacizumab, Both cells treated with Lip-Chi-Bev NPs and free Bevacizumab showed a significant decrease compared to the control cells. A 45% and 78% inhibition of cell proliferation was observed for cells treated with free Bevacizumab and Lip-Chi-Bev NPs at the highest concentration (1.25 mg / ml), respectively (Fig. 7).

3.6 The effect of Lip-Chi-Bev NPs on in vitro angiogenesis

A three-dimensional culture medium consisting of HBMEC cells was used as an in vitro model to evaluate the effects of Lip-Chi NPs, free Bevacizumab, and Lip-Chi-Bev NPs on angiogenesis. After 48 hours of cell treatment, photos were taken and the number of the formed tubular vascular branches was compared. No significant difference was observed between the number of the tubular vascular branches formed by untreated cells and cells treated with Lip-Chi NPs. Compared to these two cell groups, nevertheless, a significant decrease was observed in the number of tubular vascular branches formed by cells treatment with free Bevacizumab or Lip-Chi-Bev NPs. The suppressor effect of Lip-Chi-Bev NPs on the in vitro vascular branching was significantly greater than that of free Bevacizumab. Cell treatment with free Bevacizumab and Lip-Chi-Bev NPs resulted respectively in 26% and 58% decrease in vascular branching at a concentration of 0.725 mg/ml and 27% and 74% decrease at a concentration of 1.25 mg /ml, compared to control cells. (Figs. 8).

3.7 The effect of Lip-Chi-Bev NPs on in vivo angiogenesis

The chicken chorioallantoic membrane (CAM) model was used to evaluate the effect of Lip-Chi-Bev NPs on in vivo angiogenesis. Our in vivo findings in angiogenesis study were consistent with those obtained from our in vitro study. No significant difference was observed between the control cell groups. Nevertheless, free Bevacizumab and Lip-Chi-Bev NPs exerted a suppressor effect on in vivo angiogenesis, which were respectively calculated to be 50% and 93% compared with the untreated cell group. Thus, Lip-Chi-Bev NPs inhibited in vivo angiogenesis more effectively than free Bevacizumab (Figs. 9 and 10).

4. Discussion

Inhibition of angiogenesis and the vital involved pathways are still important challenging questions in the prevention and treatment of many diseases such as cardiovascular disease [32], corneal neovascularization [33] and cancer [34]. Despite many efforts in this field, angiogenesis is the leading cause of death in many malignancies. Anti-angiogenic therapeutic strategies are still at the beginning of the path of development and have been associated with severe side effects in many cases [35]. Therefore, emerging novel anti-angiogenic strategies or developing available therapies can be promising for the treatment of many angiogenesis-related diseases.

Cutaneous malignant melanoma is fastest-growing cancer in white populations with a large majority of dermal cancer death. Bevacizumab, a humanized anti-angiogenic immunoglobulin IgG1, is commonly

used to inhibit angiogenesis in cutaneous malignant melanoma [36]. Bevacizumab binds to vascular endothelial growth factor (VEGF-A) to block the interaction between VEGF-A and its tyrosine kinase receptor. VEGF-A is a potent stimulant of vascular endothelial cell angiogenesis by activating downstream intracellular signaling pathways leading to proliferation, migration, and sprouting of endothelial cells. Therefore, Bevacizumab offers a potential treatment for angiogenesis-related diseases by inhibiting VEGF-A signaling. However, its systemic administration has been associated with a variety of side effects in many cases [13]. Also, decreased skin absorption, reduced half-life, impaired protein structure, degradation by environmental enzymes, and loss of bioactivity are some of the challenges of local administration of Bevacizumab. To overcome some of these challenges, Bovisizumab encapsulation in nanocarriers has been reported in a variety of studies.

In this study, chitosan polymer-based lipid-coated nanoparticles were designed and synthesized with the aim of local administration of Bevacizumab. The large size of Bevacizumab limits its diffusion transport from NPs. Diffusion transport and release rate is widely associated with the rate of polymer degradation, which is influenced by various factors including the physicochemical characteristics of the polymer, mechanisms related to hydrolysis and enzymatic cleavage of the polymer. Chitosan has attracted a lot of attention in the manufacture of carriers for in vivo drug release, due to its biocompatibility and biodegradability[31], non-toxicity[37], high absorption capacity[38], availability, cost-effectiveness, and antimicrobial[39] and antioxidant[40] properties. In addition, the safety of using chitosan in food and medicine has been approved by the US Food and Drug Administration (FDA).

Here, Lip-Chi nanoparticles were successfully synthesized and used to encapsulate Bevacizumab. In a study by Parisa Badiei et al., the amount of loaded Bevacizumab and the encapsulation efficiency were reported 67% and 15%, respectively [41]. Our results showed an increase in the mentioned parameters which may be due to the change in the exposure time of Bevacizumab with chitosan, increased Bevacizumab concentration, and decreased chitosan concentration [42]. Compared to a study by Sousa F. et al. that used PLGA polymer to load Bevacizumab [43], our results indicated that chitosan polymer-based nanoencapsulation of Bevacizumab provided a significant increase in the rates of release and dermal absorption of the drug. Also, the amount of Bevacizumab released was greater. Methods to achieve nanoparticles typically include conditions such as suitable pH, high pressure and temperature, use of organic solvents and ionic strength, where any change may lead to structural instability, decreased bioactivity and increased immunogenicity of encapsulated monoclonal antibody. Our results showed that the bioactivity of encapsulated Bevacizumab is maintained in the synthesized Lip-Chi nanoparticles.

Our observations in the study of in vitro and in vivo angiogenesis showed increased suppressor function for Bevacizumab encapsulated in Lip-Chi nanoparticles compared to free Bevacizumab. These nanoparticles appear to provide an efficient environment for maintaining the structure of Bevacizumab against enzymatic degradation and other environmental threatening factors, so that the increased suppressor function of encapsulated Bevacizumab on both in vitro and in vivo angiogenesis may also be due to the release of the drug in greater amount and speed, and may also be due to better preservation of the drug structure until its release and also after its release from Lip-Chi nanoparticles[44, 45]. There are

various reports indicating the inhibitory effects of Bevacizumab on angiogenesis using cultured human endothelial cells in vitro. Here, the biological activity of Bevacizumab was determined by its capacity to suppress the endothelial cell proliferation, in vitro and in vivo tubulogenesis. Decreased proliferation and tubulogenesis indicate that Bevacizumab bioactivity was maintained even when encapsulated into Lip-Chi nanoparticles[46, 47]. MTT results also showed that Lip-Chi nanoparticles were not cytotoxic for hBMEC cells, which is consistent with previous reports.

Moreover, the observed increase in dermal absorption of Bevacizumab encapsulated in Lip-Chi nanoparticles may be mediated via lecithin phospholipids. This successful dermal absorption of Bevacizumab can suggest replacing systemic with local administration, which can be an effective strategy to reduce the side effects of systemic administration of Bevacizumab.

Our results suggest that encapsulation of Bevacizumab in chitosan-based lipid-coated nanoparticles is associated with an increased amount and rate of drug release, which may be preferable to other polymers, such as PLGA, where greater drug release is required in a shorter time. Various studies have shown that Bevacizumab encapsulated in PLGA-based nanoparticles exhibits a slow, pH-dependent release profile. Although slow release of the drug may reduce the frequency of administration, it must be proven that the nanoparticle allows the drug to be released even at a slow rate. Our results indicated that the Lip-Chi nanoparticles provide better conditions for more efficient function of Bevacizumab by increasing the efficiency of encapsulation and drug loading as well as dermal cell absorption. The use of these nanoparticles seems to be an effective strategy for local administration of Bevacizumab especially in accessible angiogenesis-related diseases such as cutaneous melanoma.

5. Conclusion

In this study, we synthesized a lipid-polymer nanoparticle that was capable of loading Bevacizumab well. Our findings showed that the anti-angiogenic effects of Bevacizumab did not change with the encapsulation process. Having anti-angiogenic effects indicates that the natural structure of Bevacizumab did not impair after encapsulation in lipid-chitosan nanoparticles and it is fully maintained until release and after its release from nanoparticles. The findings of this study confirm well that the use of Lip-Chi-Bev NPs can increase the anti-angiogenic effect and skin- absorption of bevacizumab. Based on the findings of in vitro experimental, we predict that topical administration of bevacizumab may lead to inhibition of angiogenesis in disorders such as cutaneous melanoma. The results obtained in this study confirm the necessity of studying the in vivo effect of Lip-Chi-Bev NPs.

Abbreviations

VEGF: Vascular Endothelial Growth Factor , bFGF: Fibroblast Growth Factor-b, PDGF: Platelet-Derived Growth Factor, TGFα/β: Transforming Growth Factors α and β, VEGFR-2: Tyrosine Kinase Receptor-2, TPP: Triphosphate, DLS: Dynamic Light Scattering, PDI: Polydispersity index, SEM: Scanning Electron Microscopy, FTIR: Fourier-transform infrared spectroscopy, CAM assay: Chorioallantoic Membrane Assay

Declarations

Conflict of interest

All authors confirm that there is no any declaration of interests.

6. Acknowledgments

The authors gratefully acknowledge the research council of Kermanshah University of Medical Sciences (Grant Number. 990062) for financial support. This work was performed in partial fulfillment of the requirement for M.Sc. Nanomedicine of Fereshteh Abdi, in the faculty of Pharmacy, Kermanshah University of Medical Sciences, Kermanshah, Iran.

References

1. Carr S, Smith C, Wernberg J. Epidemiology and Risk Factors of Melanoma. Surg Clin North Am. 2020;100(1):1–12. DOI:https://doi.org/10.1016/j.suc.2019.09.005.
2. Spanogle JP, et al. Risk of second primary malignancies following cutaneous melanoma diagnosis: a population-based study. J Am Acad Dermatol. 2010;62(5):757–67. DOI:https://doi.org/10.1016/j.jaad.2009.07.039.
3. Nishida N, et al. Angiogenesis in cancer. Vasc Health Risk Manag. 2006;2(3):213. DOI:https://doi.org/10.2147/vhrm.2006.2.3.213.
4. Mahabeleshwar GH, Byzova TV. *Angiogenesis in melanoma*. in *Semin Oncol*. Elsevier; 2007.
5. Kliche S, Waltenberger J. VEGF receptor signaling and endothelial function. IUBMB Life. 2001;52(1):61–6. DOI:https://doi.org/10.1080/15216540252774784.
6. Stacker SA, Achen MG. The VEGF signaling pathway in cancer: the road ahead. Chin J cancer. 2013;32(6):297. DOI:https://doi.org/10.5732/cjc.012.10319.
7. Emmett MS, Dewing D, Pritchard-Jones RO. Angiogenesis and melanoma-from basic science to clinical trials. Am J Cancer Res. 2011;1(7):852.
8. Tol J, et al. Gastrointestinal ulceration as a possible side effect of bevacizumab which may herald perforation. Invest New Drugs. 2008;26(4):393–7.
9. Economopoulou P, et al. Cancer therapy and cardiovascular risk: focus on bevacizumab. Cancer Manag Res. 2015;7:133. DOI:https://doi.org/10.2147/CMAR.S77400.
10. Totzeck M, Mincu RI, Rassaf T. Cardiovascular adverse events in patients with cancer treated with bevacizumab: a meta-analysis of more than 20 000 patients. J Am Heart Assoc. 2017;6(8):e006278.
11. Rasier R, et al. The effect of intravitreal bevacizumab (avastin) administration on systemic hypertension. Eye. 2009;23(8):1714–8. DOI:https://doi.org/10.1038/eye.2008.360.
12. Nalluri SR, et al. Risk of venous thromboembolism with the angiogenesis inhibitor bevacizumab in cancer patients: a meta-analysis. JAMA. 2008;300(19):2277–85. DOI:https://doi.org/10.1001/jama.2008.656.

13. Taugourdeau-Raymond S, et al. Bevacizumab-induced serious side-effects: a review of the French pharmacovigilance database. Eur J Clin Pharmacol. 2012;68(7):1103–7. DOI:https://doi.org/10.1007/s00228-012-1232-7.
14. Letarte N, Bressler LR, Villano JL. Bevacizumab and central nervous system (CNS) hemorrhage. Cancer Chemother Pharmacol. 2013;71(6):1561–5. DOI:https://doi.org/10.1007/s00280-013-2155-4.
15. Mailliez A, et al. Nasal septum perforation: a side effect of bevacizumab chemotherapy in breast cancer patients. Br J Cancer. 2010;103(6):772–5. DOI:https://doi.org/10.1038/sj.bjc.6605828.
16. Schäfer-Korting M, Mehnert W, Korting H-C. Lipid nanoparticles for improved topical application of drugs for skin diseases. Adv Drug Deliv Rev. 2007;59(6):427–43.
17. Garcês A, et al. Formulations based on solid lipid nanoparticles (SLN) and nanostructured lipid carriers (NLC) for cutaneous use: A review. Eur J Pharm Sci. 2018;112:159–67.
18. Kirjavainen M, et al. Liposome–skin interactions and their effects on the skin permeation of drugs. Eur J Pharm Sci. 1999;7(4):279–86.
19. Elnaggar YS, et al. Lecithin-based nanostructured gels for skin delivery: an update on state of art and recent applications. J Control Release. 2014;180:10–24. DOI:https://doi.org/10.1016/j.jconrel.2014.02.004.
20. Ehterami A, et al. In vitro and in vivo study of PCL/COLL wound dressing loaded with insulin-chitosan nanoparticles on cutaneous wound healing in rats model. Int J Biol Macromol. 2018;117:601–9. DOI:https://doi.org/10.1016/j.ijbiomac.2018.05.184.
21. Stie MB, et al. Delivery of proteins encapsulated in chitosan-tripolyphosphate nanoparticles to human skin melanoma cells. Colloids Surf B Biointerfaces. 2019;174:216–23. DOI:https://doi.org/10.1016/j.colsurfb.2018.11.005.
22. Calvo P, et al. Novel hydrophilic chitosan-polyethylene oxide nanoparticles as protein carriers. J Appl Polym Sci. 1997;63(1):125–32.
23. Abdi F, et al. Interactions of Bevacizumab with chitosan biopolymer nanoparticles: Molecular modeling and spectroscopic study. J Mol Liq. 2021;339:116655. DOI:https://doi.org/10.1016/j.molliq.2021.116655.
24. Mortazavi-Jahromi SS, et al. Anti-diabetic effect of β-D-mannuronic acid (M2000) as a novel NSAID with immunosuppressive property on insulin production, blood glucose, and inflammatory markers in the experimental diabetes model. Arch Physiol Biochem. 2019;125(5):435–40.
25. Seyfi P, et al. In vitro and in vivo anti-angiogenesis effect of shallot (Allium ascalonicum): a heat-stable and flavonoid-rich fraction of shallot extract potently inhibits angiogenesis. Toxicol In Vitro. 2010;24(6):1655–61. DOI:https://doi.org/10.1016/j.tiv.2010.05.022.
26. Cai J, et al. Preparation and evaluation of lipid polymer nanoparticles for eradicating H. pylori biofilm and impairing antibacterial resistance in vitro. Int J Pharm. 2015;495(2):728–37. DOI:https://doi.org/10.1016/j.ijpharm.2015.09.055.
27. Kuesters GM, Campbell RB. Conjugation of bevacizumab to cationic liposomes enhances their tumor-targeting potential. Nanomedicine. 2010;5(2):181–92.

28. Ugurlu N, et al. Transscleral delivery of bevacizumab-loaded chitosan nanoparticles. J Biomed Nanotechnol. 2019;15(4):830–8.
29. Sonvico F, et al. Formation of self-organized nanoparticles by lecithin/chitosan ionic interaction. Int J Pharm. 2006;324(1):67–73. DOI:https://doi.org/10.1016/j.ijpharm.2006.06.036.
30. Rodrigues LR, Jose J. Exploring the photo protective potential of solid lipid nanoparticle-based sunscreen cream containing Aloe vera. Environ Sci Pollut Res. 2020;27(17):20876–88. DOI:https://doi.org/10.1007/s11356-020-08543-4.
31. Bakshi PS, et al. Chitosan as an environment friendly biomaterial–a review on recent modifications and applications. Int J Biol Macromol. 2020;150:1072–83.
32. Zachary I, Morgan RD. Therapeutic angiogenesis for cardiovascular disease: biological context, challenges, prospects. Heart. 2011;97(3):181–9. DOI:https://doi.org/10.1136/hrt.2009.180414.
33. Chang JH, et al., Corneal neovascularization: an anti-VEGF therapy review. Surv Ophthalmol, 2012. 57(5): p. 415 – 29 DOI: https://doi.org/10.1016/j.survophthal.2012.01.007.
34. Rajabi M, Mousa SA. The role of angiogenesis in cancer treatment. Biomedicines. 2017;5(2):34. DOI:https://doi.org/10.3390/biomedicines5020034.
35. Tarallo V, De Falco S. The vascular endothelial growth factors and receptors family: Up to now the only target for anti-angiogenesis therapy. Int J Biochem Cell Biol. 2015;64:185–9. DOI:https://doi.org/10.1016/j.biocel.2015.04.008.
36. Domingues B, et al. Melanoma treatment in review. Immunotargets Ther. 2018;7:35–49. DOI:https://doi.org/10.2147/ITT.S134842.
37. Kean T, Thanou M. Biodegradation, biodistribution and toxicity of chitosan. Adv Drug Deliv Rev. 2010;62(1):3–11. DOI:https://doi.org/10.1016/j.addr.2009.09.004.
38. Zahiri M, et al. Encapsulation of curcumin loaded chitosan nanoparticle within poly (ε-caprolactone) and gelatin fiber mat for wound healing and layered dermal reconstitution. Int J Biol Macromol. 2020;153:1241–50.
39. Divya K, et al. Antimicrobial properties of chitosan nanoparticles: Mode of action and factors affecting activity. Fibers Polym. 2017;18(2):221–30.
40. Vinsova J, Vavrikova E. Chitosan derivatives with antimicrobial, antitumour and antioxidant activities-a review. Curr Pharm Des. 2011;17(32):3596–607.
41. Badiee P, et al. Ocular implant containing bevacizumab-loaded chitosan nanoparticles intended for choroidal neovascularization treatment. J Biomed Mater Res A. 2018;106(8):2261–71. DOI:https://doi.org/10.1002/jbm.a.36424.
42. Gan Q, Wang T. Chitosan nanoparticle as protein delivery carrier—systematic examination of fabrication conditions for efficient loading and release. Colloids Surf B Biointerfaces. 2007;59(1):24–34.
43. Sousa F, et al. A new paradigm for antiangiogenic therapy through controlled release of bevacizumab from PLGA nanoparticles. Sci Rep. 2017;7(1):1–13.

44. Solaro R, Chiellini F, Battisti A. Target delivery protein drugs nanocarriers Mater. 2010;3(3):1928–80.
45. Dziubla TD, Karim A, Muzykantov VR. Polymer nanocarriers protecting active enzyme cargo against proteolysis. J Control Release. 2005;102(2):427–39. DOI:https://doi.org/10.1016/j.jconrel.2004.10.017.
46. Sun J-G, et al. Mesoporous silica nanoparticles as a delivery system for improving antiangiogenic therapy. Int J Nanomedicine. 2019;14:1489.
47. de Redín IL, et al. In vivo effect of bevacizumab-loaded albumin nanoparticles in the treatment of corneal neovascularization. Exp Eye Res. 2019;185:107697.

Figures

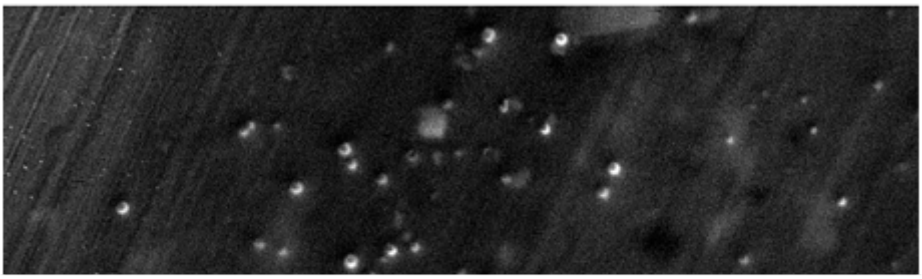

Figure 1

Scanning electron microscopy (SEM) image of Lip-Chi-Bev NPs.

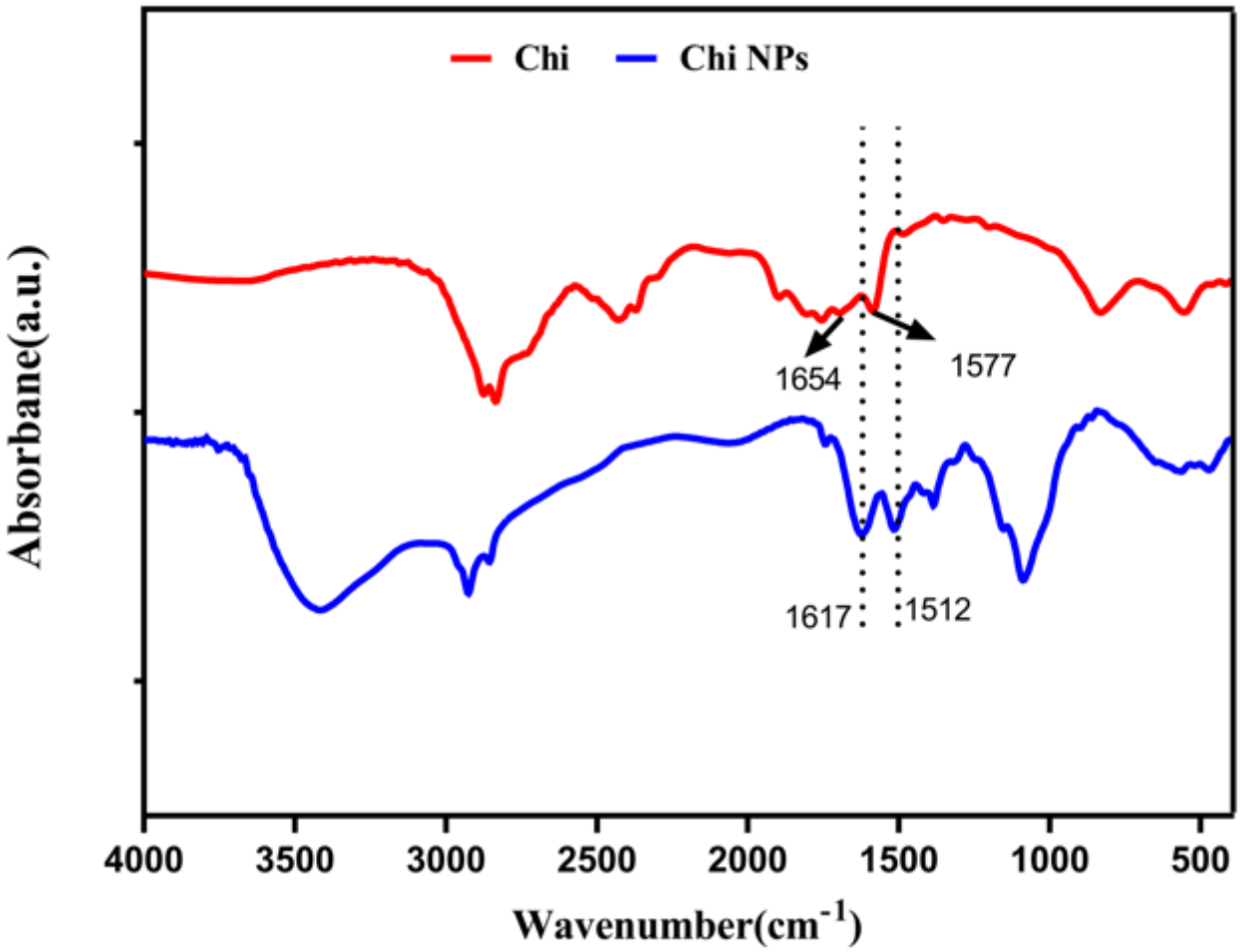

Figure 2

The FTIR spectra of chitosan and Chi-Bev NPs.

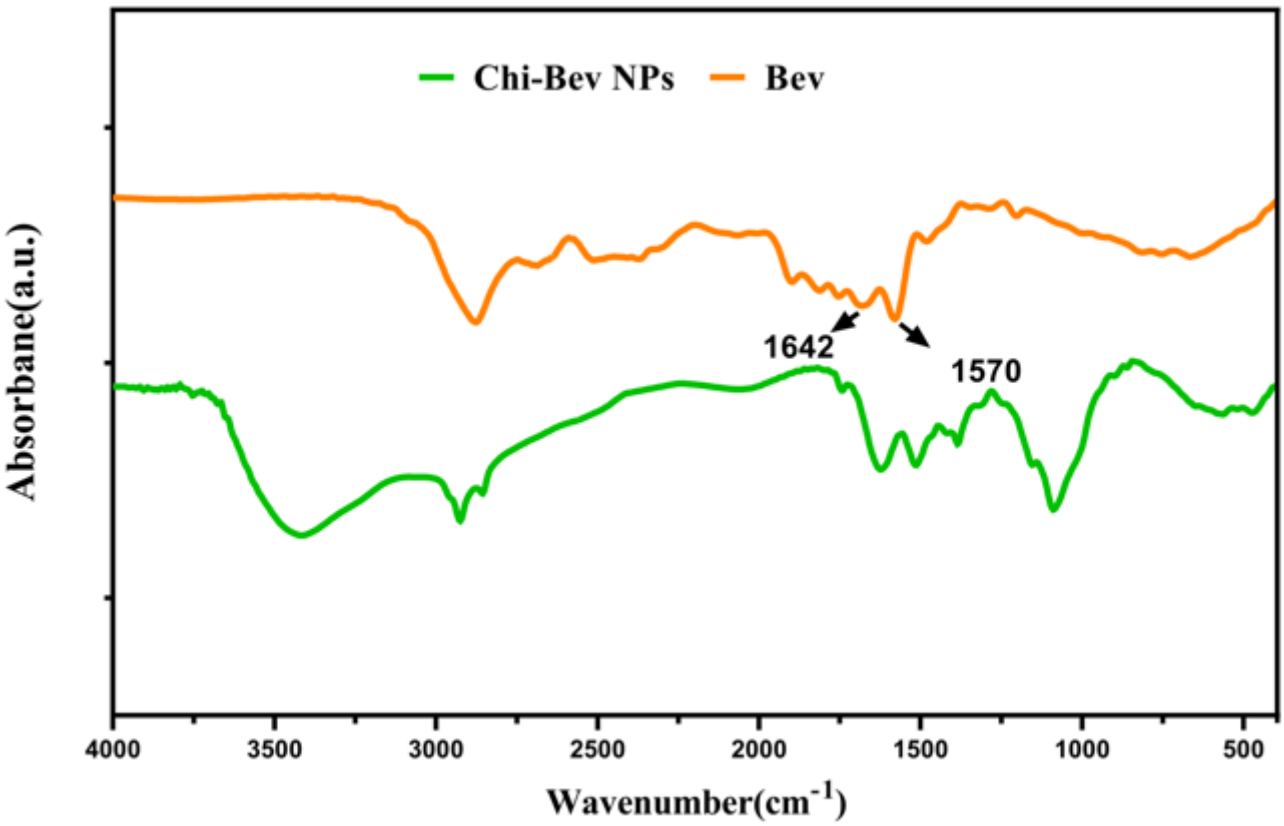

Figure 3

The FTIR spectra of Bevacizumab and Chi-Bev NPs.

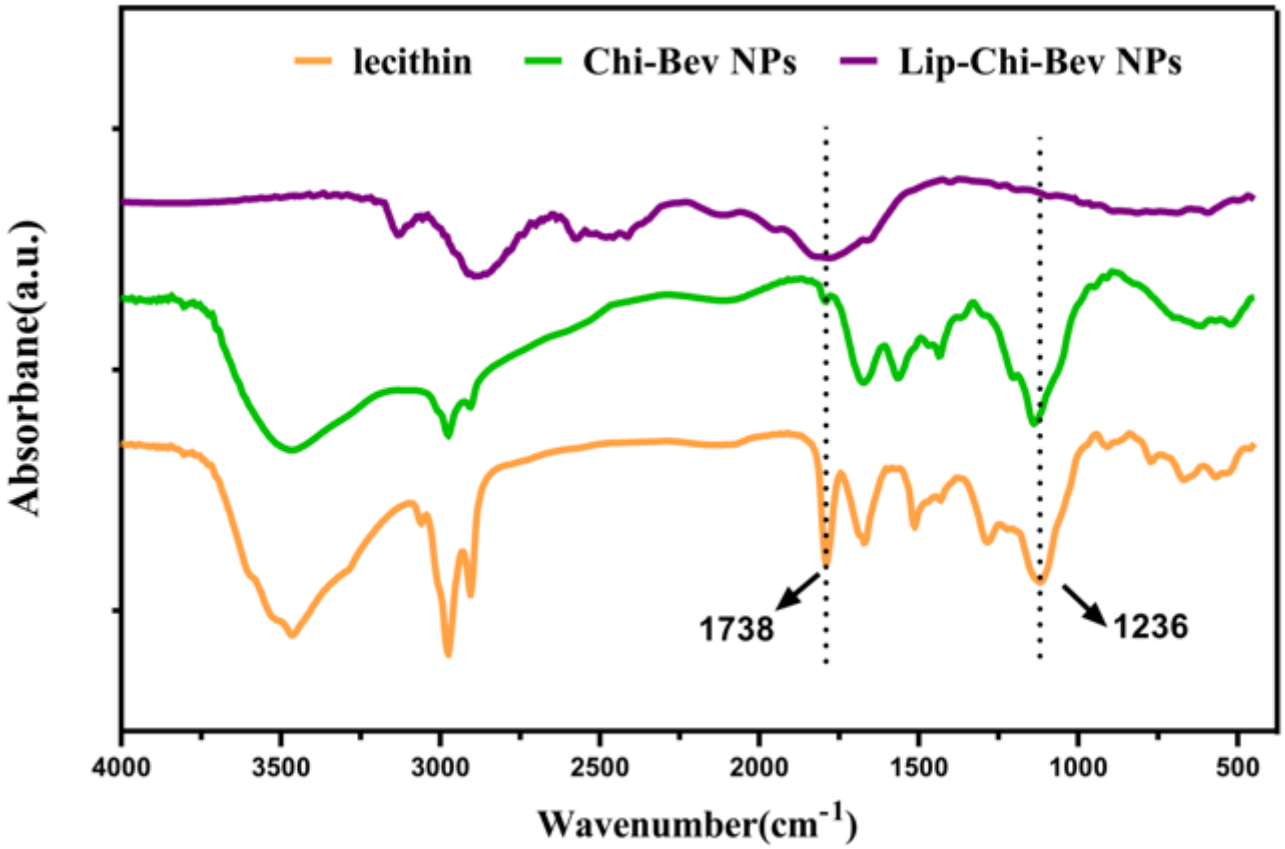

Figure 4

The FTIR spectra of Lecithin, Lip-Chi-Bev NPs, and Chi-Bev NPs.

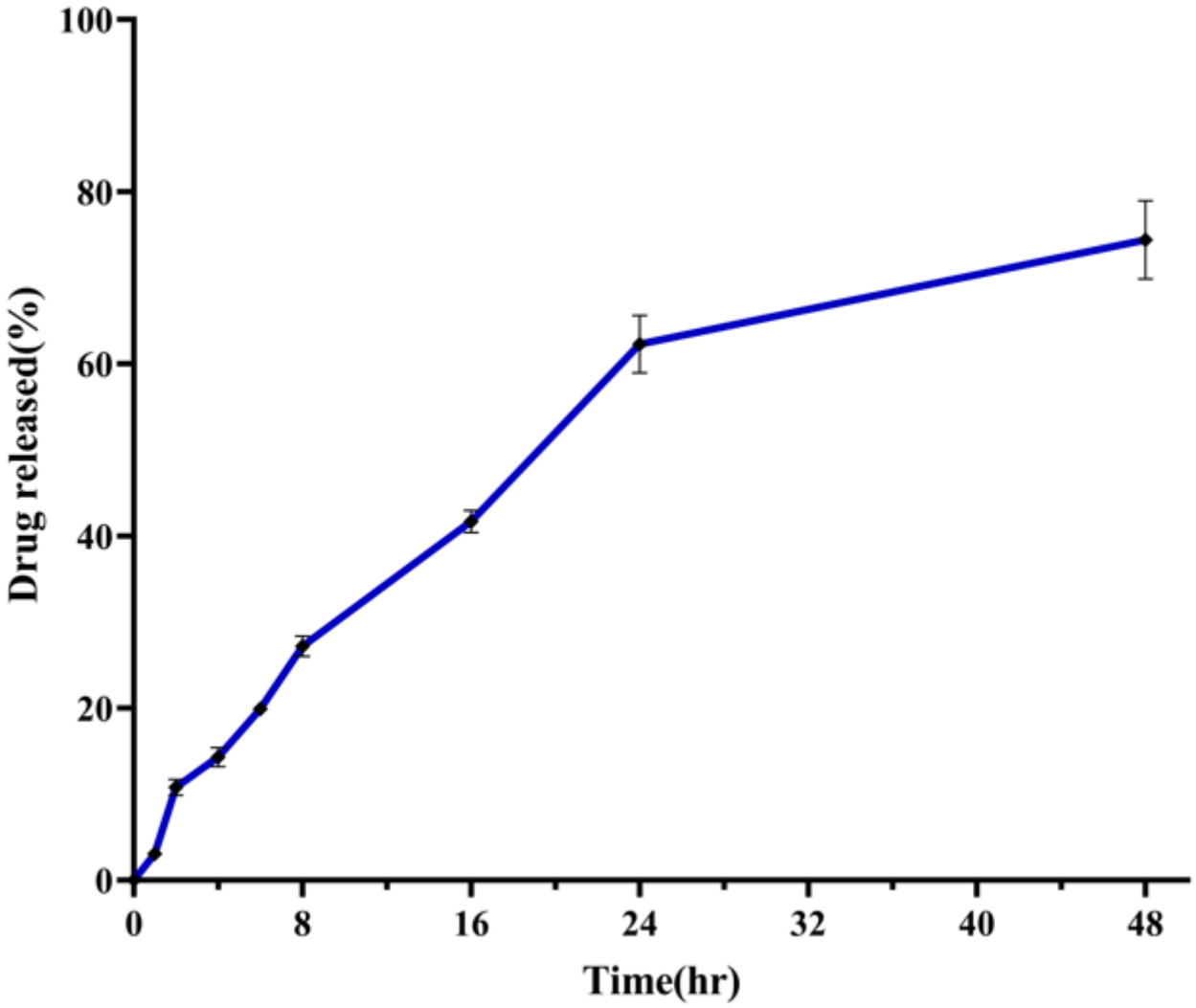

Figure 5

Drug release profile of Lip-Chi-Bev NPs.

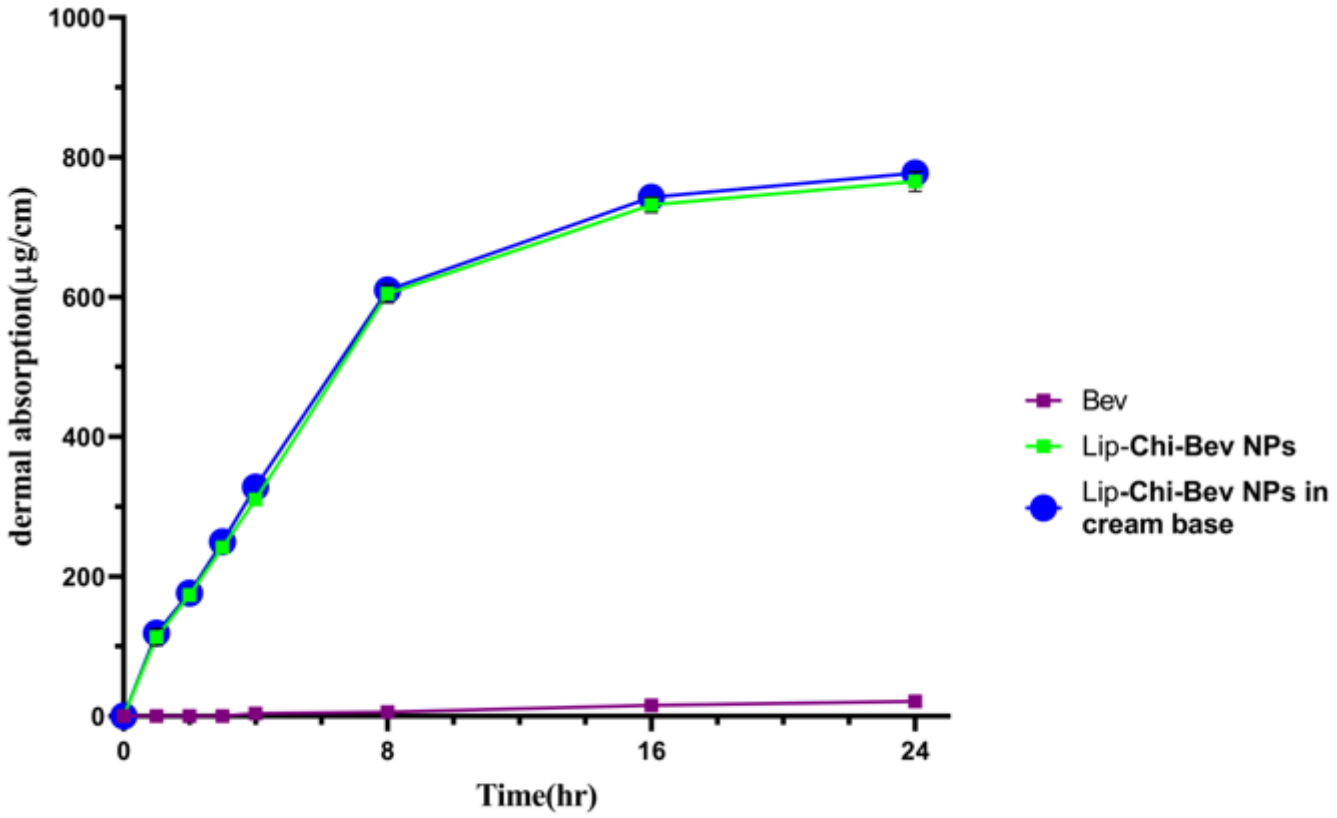

Figure 6

Dermal absorption of Lip-Chi-Bev NPs in cream base, Lip-Chi-Bev NPs and free Bevacizumab.

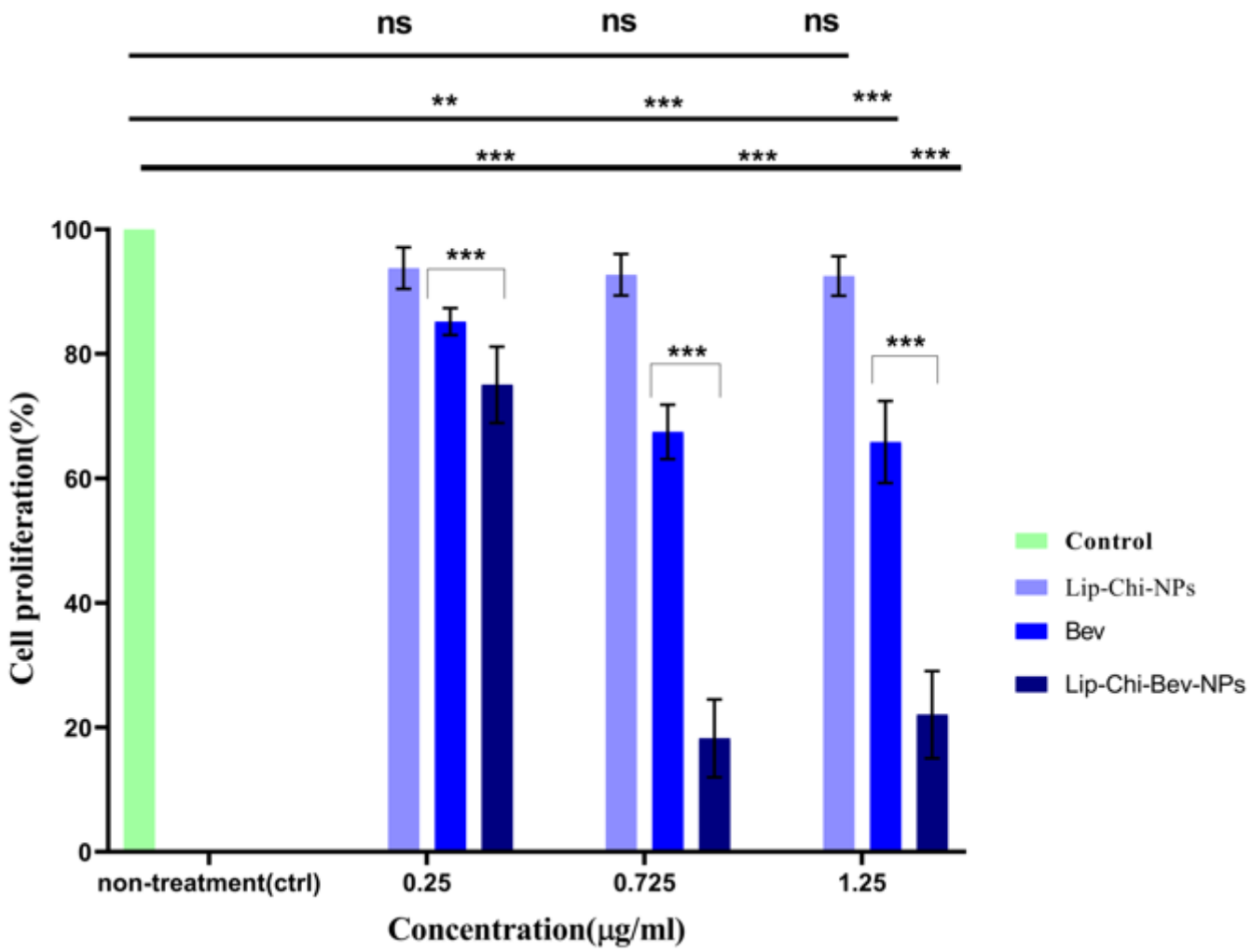

Figure 7

MTT results showed decreased endothelial cell proliferation under treatment of Lip-Chi-Bev NPs, more concentrations led to more decrease in cell proliferation.

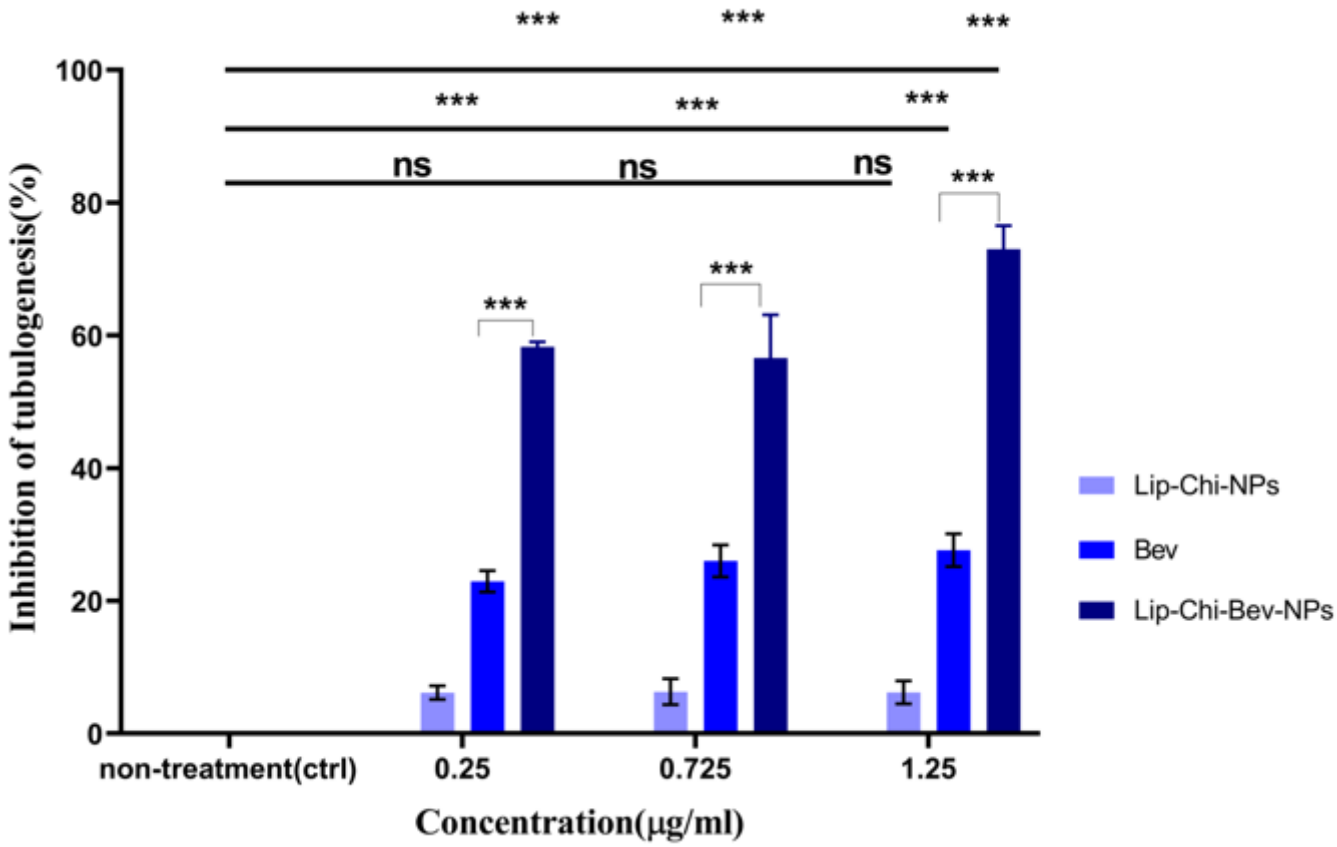

Figure 8

In vitro tubulogenesis assay showed inhibitory effects of Lip-Chi-Bev NPs on endothelial cells angiogenesis, more concentrations led to more inhibitory effects.

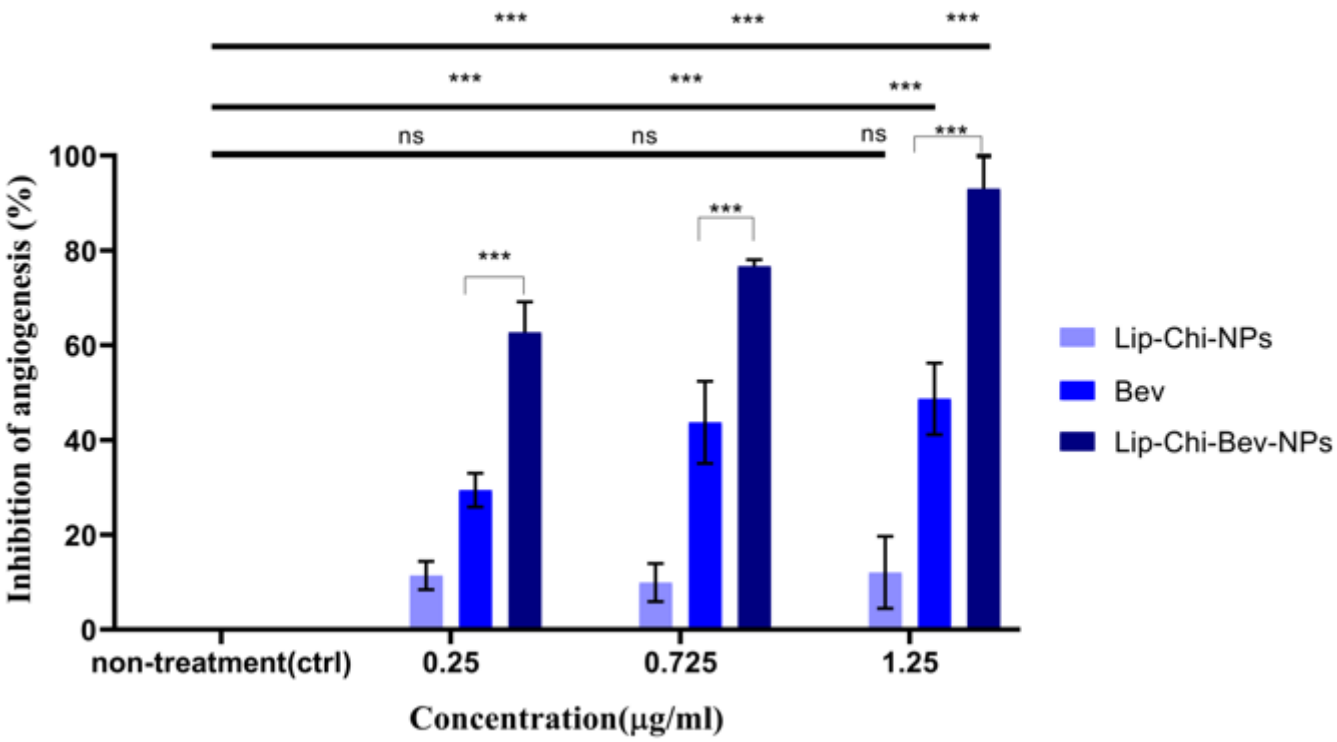

Figure 9

In vivo angiogenesis assay showed inhibitory effects of Lip-Chi-Bev NPs on angiogenesis, more concentrations led to more inhibitory effects.

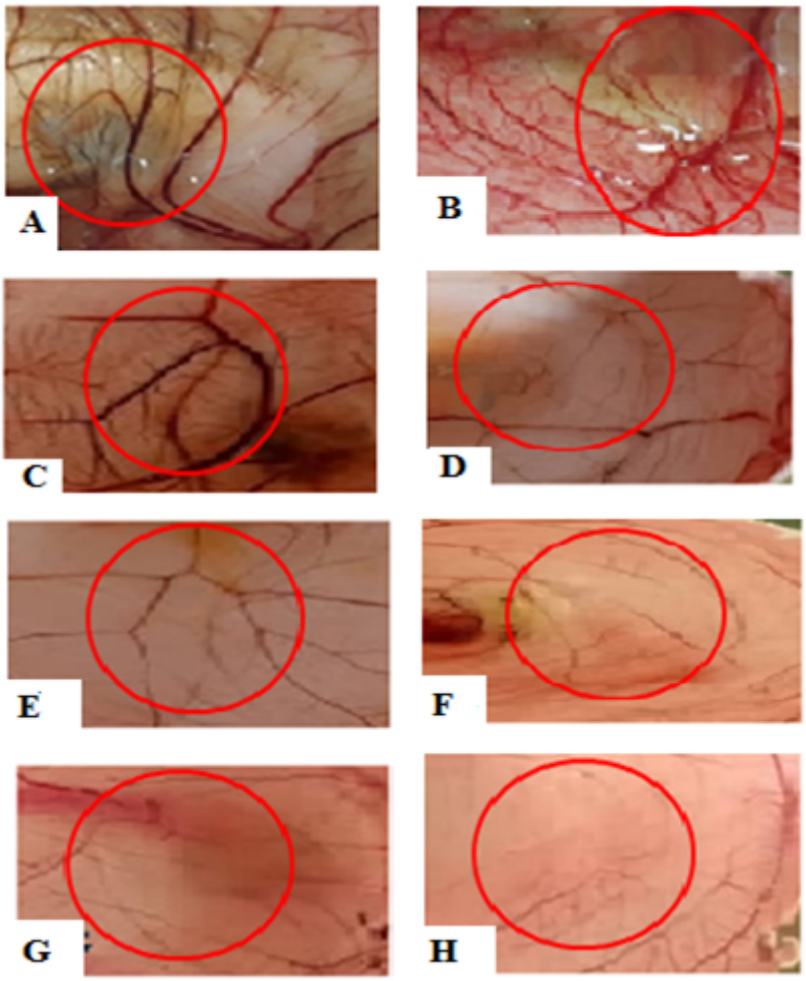

Figure 10

Result of CAM assay. Control (A). Chi-Bev NPs (B). Concentration 0.25 mg/egg (Free Bevacizumab(C) and Lip-Chi-Bev NPs (D)). Concentration 0.725 mg/egg (Free Bevacizumab (E) and Lip-Chi-Bev NPs (F)). Concentration 1.25 mg/egg (Free Bevacizumab (G) and Lip-Chi-Bev NPs (H)).

Supplementary Files

This is a list of supplementary files associated with this preprint. Click to download.

- GraphicalAbstract.png